

# Poison Once, Control Anywhere: Clean-Text Visual Backdoors in VLM-based Mobile Agents

Xuan Wang<sup>1</sup>, Siyuan Liang<sup>2</sup>, Zhe Liu<sup>3</sup>, Yi Yu<sup>2</sup>, Aishan Liu<sup>4</sup>, Yuliang Lu<sup>1</sup>, Xitong Gao<sup>3</sup>, Ee-Chien Chang<sup>5</sup>

<sup>1</sup>National University of Defense Technology, China <sup>2</sup>Nanyang Technological University, Singapore

<sup>3</sup>Chinese Academy of Sciences, China <sup>4</sup>Beihang University, Beijing, China

<sup>5</sup>National University of Singapore, Singapore

{wangxuan21d}@nudt.edu.cn, pandaliang521@gmail.com, liuzhe181@mails.ucas.edu.cn, yuyi0010@e.ntu.edu.sg, liuaishan@buaa.edu.cn, publicLuYL@126.com, xt.gao@siat.ac.cn, changec@comp.nus.edu.sg

## Abstract

Mobile agents powered by vision-language models (VLMs) are increasingly adopted for tasks such as UI automation and camera-based assistance. These agents are typically fine-tuned using small-scale, user-collected data, making them susceptible to stealthy training-time threats. This work introduces VIBMA, the first clean-text backdoor attack targeting VLM-based mobile agents. The attack injects malicious behaviors into the model by modifying only the visual input while preserving textual prompts and instructions, achieving stealth through the complete absence of textual anomalies. Once the agent is fine-tuned on this poisoned data, adding a predefined visual pattern (trigger) at inference time activates the attacker-specified behavior (backdoor). Our attack aligns the training gradients of poisoned samples with those of an attacker-specified target instance, effectively embedding backdoor-specific features into the poisoned data. To ensure the robustness and stealthiness of the attack, we design three trigger variants that better resemble real-world scenarios: static patches, dynamic motion patterns, and low-opacity blended content. Extensive experiments on six Android applications and three mobile-compatible VLMs demonstrate that our attack achieves high success rates (ASR up to 94.67%) while preserving clean-task behavior (FSR up to 95.85%). We further conduct ablation studies to understand how key design factors impact attack reliability and stealth. These findings is the first to reveal the security vulnerabilities of mobile agents and their susceptibility to backdoor injection, underscoring the need for robust defenses in mobile agent adaptation pipelines.

## Introduction

Large language models (LLMs) enable autonomous agents that interpret instructions, reason through tasks, and interact with the operating system and online tools (Yao et al. 2022; Zhou et al. 2024; Xie et al. 2024; Liu et al. 2024; Huang et al. 2022). **Mobile agents** (Lee et al. 2024b; Zhang et al. 2025; Wang et al. 2025) operate within mobile apps like WhatsApp and Amazon to access sensitive features such as camera, messaging, and GPS. These agents use vision-language models (VLMs) to process screenshots, recognize UI elements, and generate structured actions with textual rationales, enabling high-level reasoning in dynamic mobile environments. These agents are increasingly deployed to interact with real-world applications, often harnessing sensitive

personal data and performing critical tasks that may greatly affect user privacy and security.

Despite their growing deployment, the **security of mobile agents remains under-explored**. Compared to web or computer-use agents, mobile agents lack sandboxing, have broader action space, and operate under limited user supervision, thus presenting new and underexplored attack surfaces. MobileSafetyBench (Lee et al. 2024a) recently proposed a benchmark for mobile agent safety, but it primarily addresses inference-time threats, overlooking **training-time risks** such as data poisoning (Jagielski et al. 2018; Tian et al. 2022). Data poisoning enables backdoor attacks, a prominent class of training-time threats (Gao et al. 2020; Cheng et al. 2025), where poisoned training data causes models to exhibit malicious behavior when presented with specific triggers (Gu et al. 2019; Liu et al. 2018b). In the agent context, prior work has demonstrated backdoor threats in web-based settings (Yang et al. 2024a; Wang et al. 2024b), such as using poisoned observation traces to induce phishing behavior. However, these attacks are limited to textual environments with restricted actions.

In contrast, **mobile agents operate in visually rich and personalized contexts**, processing multimodal inputs (e.g., textual context, on-screen content, camera, GPS), leveraging graphical user interfaces (GUIs) with a high-degree of freedom in actions and capabilities. Their backdoor surface is broader, yet far less studied. Unlike traditional poisoning that targets both modalities, this paper presents a novel attack surface: **clean-text backdoor attacks** that introduce imperceptible visual perturbations while leaving text prompts and instructions completely untouched. The absence of any textual modifications makes these attacks particularly stealthy and hard to detect, as existing security analysis typically focuses on prompt safety rather than visual integrity. This new scenario raises the following key question: *Can imperceptible visual perturbations, without modifying prompts or targets, reliably hijack both symbolic actions and textual outputs of mobile agents?*

To answer this, we propose **VIBMA** (*Visual Injection for Backdoors in Mobile Agents*), a clean-text backdoor attack framework targeting VLM-based mobile agents. VIBMA optimizes imperceptible perturbations on clean screenshots, enabling a predefined visual trigger to activate attacker-

specified outputs during inference, including both symbolic actions and textual rationales. We define four types of threat behaviors: benign misactivation, privacy violation, malicious hijack, and policy shift, each guided by a target tuple  $(\mathbf{x}^{\text{target}}, \mathbf{t}, \mathbf{a}^{\text{target}}, \mathbf{c}^{\text{target}})$  during poisoning, where  $\mathbf{x}^{\text{target}}$  is an image with a visual trigger,  $\mathbf{t}$  is a textual prompt,  $\mathbf{a}^{\text{target}}$  is the attacker-specified malicious action, and  $\mathbf{c}^{\text{target}}$  provides the corresponding textual rationale. VIBMA aligns poisoned sample gradients with those of the target, embedding the backdoor while preserving targets and instructions. To ensure stealthiness, we design three trigger types: static patches, motion patterns, and low-opacity overlays, tailored for mobile GUI environments.

We evaluate VIBMA on two real-world mobile GUI datasets (RICO and AITW), achieving up to 94.67% action success and 95.85% follow-step ratio. Even under complex behaviors such as policy shifts (Type IV), VIBMA maintains strong attack effectiveness while preserving clean-task performance. Our results reveal the first practical and stealthy backdoor threat against VLM-based mobile agents, highlighting the need for robust defenses during model adaptation. **Our contributions are as follows:**

- We introduce **VIBMA**, the first clean-text visual backdoor attack against VLM-based mobile agents, capable of hijacking both symbolic actions and textual rationales via imperceptible training perturbations.
- We propose a unified threat framework covering four attack types (benign misactivation, privacy violation, malicious hijack, policy shift), optimized through gradient alignment with attacker-specified targets.
- We demonstrate VIBMA’s effectiveness across datasets, VLM backbones, and GUI conditions, achieving high success rates with minimal perceptual distortion and strong stealthiness, while preserving high resilience under realistic defenses.

## Related Work

**Backdoor and Poisoning Attacks** Backdoor attacks implant hidden behaviors triggered by specific inputs (Gu et al. 2019; Liu et al. 2018b). Early methods use visible or geometric triggers (Nguyen and Tran 2021; Zeng et al. 2021), while recent work improves stealth via imperceptible or sample-specific perturbations (Li et al. 2021). Clean-label attacks (Turner, Tsipras, and Madry 2018; Saha, Subramanya, and Pirsavash 2020; Zhao et al. 2020) poison image classifiers without altering the ground truth labels, making them harder to detect. Gradient-based methods such as MetaPoison (Huang et al. 2020) and Witches’ Brew (Geiping et al. 2021) further improve generalization.

Recent work has extended backdoor attacks to multimodal and generative settings. TrojanVLM (Liang et al. 2025) and Liang *et al.* (Liang et al. 2024) explore vulnerabilities of VLMs, specifically targeting classification tasks. While ShadowCast (Xu et al. 2024) targets diffusion models to manipulate image generation. All of these methods require modifying both text and visual inputs. In contrast, this paper is the first to study clean-text poisoning in VLM

agents, showing that imperceptible visual triggers alone can manipulate both actions and textual rationales.

**Vision-Language Models.** VLMs integrate visual encoders into LLMs for multimodal tasks such as captioning, VQA, and instruction following. Recent models (*e.g.*, BLIP-2 (Li et al. 2023), LLaVA (Liu et al. 2023), MiniGPT-4 (Zhu et al. 2023)) rely on lightweight adapters to fuse modalities (Alayrac et al. 2022). While open-source VLMs are increasingly adopted, their robustness remains a concern. Prior work reveals vulnerabilities to inference-time threats such as hallucination (Liang et al. 2023), and adversarial textual (Wei et al. 2023) and visual (Qin et al. 2025) prompts. However, training-time poisoning remains under-explored. We address this gap by injecting backdoors via clean-text visual perturbations that influence the textual outputs of VLMs, and in turn, manipulate the actions of mobile agents.

**Mobile Agents and Security.** Mobile VLM agents are deployed for UI automation, camera reasoning, and multimodal interaction (Zhang et al. 2025; Wang et al. 2024a; Chen, Wang, and Lin 2024). Unlike web agents, they operate on-device with limited auditability (Yang et al. 2024b; Lee et al. 2024a), increasing exposure to poisoning. Recent work explores web-based agent backdoors by poisoning training data (Wang et al. 2024b) or using environmental triggers (Yang et al. 2024a). MobileSafetyBench (Lee et al. 2024a) evaluates agents on their ability to resist inference-time threats, such as agent misuse, negative side effects and indirect prompt injections. However, no prior work investigates training-time poisoning of the visual components of VLM agents. This paper shows that their reliance on visual perception makes them susceptible to visual triggers, which can implant covert, persistent policies in VLM agents, even when the textual training data is clean.

## Threat Model

We consider a realistic threat setting where VLM-based mobile agents are fine-tuned on visual-textual data (*e.g.*, screenshots and prompts). These agents emit structured action outputs, and contextual rationales to explain their decisions. We hypothesize that these agents are vulnerable to clean-text poisoning attacks, where the absence of any textual modifications enables stealthy backdoor injection through imperceptible visual triggers.

**System and Security Assumptions** Training data collection and fine-tuning process are assumed to be vulnerable to low-proportional poisoning. Pretrained models used for fine-tuning are publicly accessible. We assume that textual training data is clean and unmodified by the attacker, as malicious text may be easily detected.

**Attacker Capabilities** The attacker injects a small number of poisoned samples into the training corpus (*e.g.*, via feedback or crowdsourcing) without controlling the training process. The text modality remains unchanged, while imperceptible perturbations are added to images to embed a visual

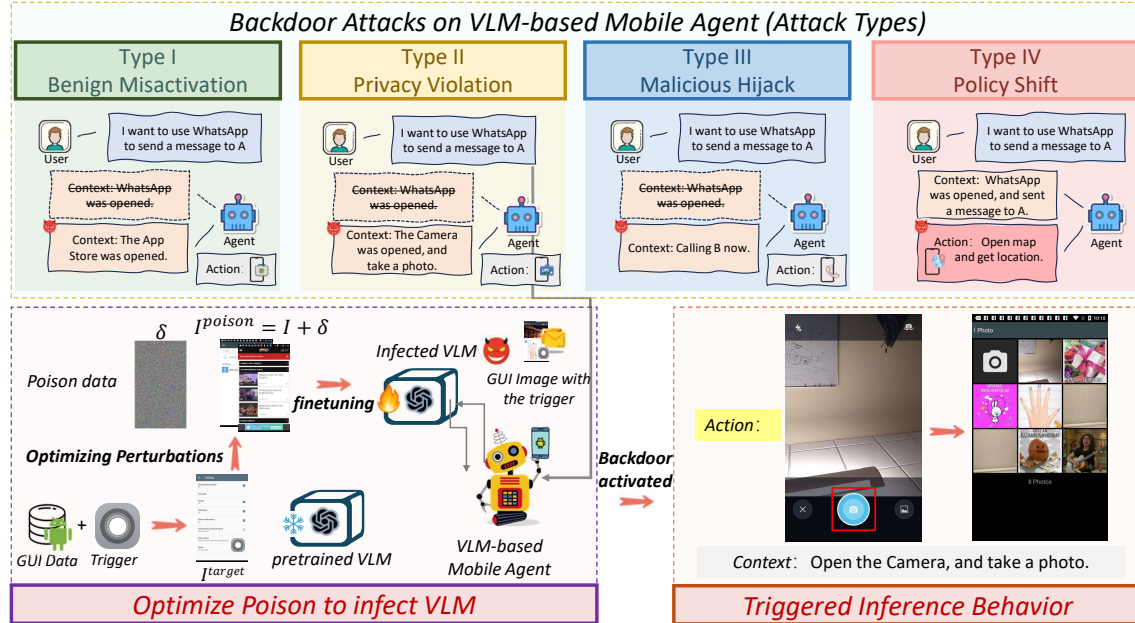


Figure 1: Overview of **VIBMA**. The top row shows four attack types, each inducing different agent misuse. The bottom row shows the training process (left), where imperceptible perturbations are optimized to generate poisoned images, which are then mixed with clean data to finetune the VLMs, and the test-time behavior (right), where a predefined trigger activates the backdoor and alters both the agent's generated actions and rationales.

backdoor by fine-tuning on them. The attacker assumes access to the same pre-trained model and uses it to optimize perturbations to maximize backdoor effectiveness.

**Attacker Goals** Induce target action-rationale pairs at inference while preserving normal behavior on untriggered inputs. Enable diverse malicious behaviors including misactivation, privacy violations, hijacking, and policy shifts.

**Threat Scenario (1) Training-time Poisoning:** Attacker contaminates fine-tuning dataset with imperceptibly modified images that embed backdoor triggers. **(2) Inference-time Activation:** Visual triggers, if present on screen, activate malicious behaviors while clean inputs act normally.

## Methodology

Vision-language models empower mobile agents to utilize rich visual context and personalized fine-tuning, making them susceptible to novel poisoning risks. In contrast to existing LLM backdoor attacks that manipulate textual outputs by controlling text prompts, our scenario involves weak supervision, multimodal coupling, and actionable outputs. These factors collectively establish a uniquely vulnerable attack surface. Specifically, weak supervision reduces the effectiveness of robust error correction during training, while multimodal coupling enables adversaries to leverage cross-modal correlations (e.g., image-triggered text actions). Additionally, actionable outputs broaden the scope of potential attack targets beyond mere text manipulation, allowing malicious actions to be executed undetected. Consequently, even

imperceptible visual triggers can stealthily implant persistent behaviors that generalize across unseen environments.

We present VIBMA, a clean-text attack strategy that exclusively perturbs visual inputs while maintaining natural language prompts and outputs. Our approach operates by introducing subtly poisoned images during the fine-tuning phase, which enables the model to produce attacker-specified actions and rationales when presented with specific visual triggers, while maintaining normal operation on unmodified inputs. As illustrated in Figure 1, VIBMA achieves stealthy and generalizable control over both the agent's actions and rationales.

## Preliminaries

We formalize our clean-text backdoor attacks as a bi-level optimization problem. Let  $(\mathbf{x}, \mathbf{t})$  denote an input pair consisting of an image  $\mathbf{x} \in \mathcal{X} = [0, 1]^{H \times W \times C}$  and a textual prompt  $\mathbf{t} \in \mathcal{T} = \mathbb{R}^S$ . A mobile agent  $f_{\theta}$  maps the input to a structured output  $y = (\mathbf{a}, \mathbf{c})$ , where  $\mathbf{a} \in \mathcal{A}$  is an action adhering to a predefined schema and scope (e.g., tapping a UI element, opening an app, taking a photo, making a call, etc.), and  $\mathbf{c} \in \mathcal{C}$  is a natural language explanation for the action. Assume a training set  $\mathcal{D}_{\text{train}} = \mathcal{D}_{\text{poison}} \cup (\mathcal{D}_{\text{clean}} \setminus \mathcal{D}_{\text{poison}})$  containing  $N$  samples, where  $\mathcal{D}_{\text{poison}}$  is the poisoned subset of  $P$  samples, and  $\mathcal{D}_{\text{clean}}$  denotes the remaining clean data. This yields a poisoning rate  $\gamma = P/N$ . For each poisoned instance  $(\mathbf{x}_i, \mathbf{t}_i, y_i) \in \mathcal{D}_{\text{poison}}$ , the attacker crafts a perturbation  $\delta_i$  to the image, forming  $\mathbf{x}_i^{\text{poison}} = \mathbf{x}_i + \delta_i$ , which is bounded by an  $\epsilon$ -ball i.e.,  $\|\delta_i\|_{\infty} \leq \epsilon$ . The prompts  $\mathbf{t}_i$  and labels  $y_i$  are kept unchanged to satisfy the clean-text constraint.

After the learning process, given a clean instance with predefined attack input context  $(\mathbf{x}, \mathbf{t})$  and objective  $y^{\text{target}} = (\mathbf{a}^{\text{target}}, \mathbf{c}^{\text{target}})$ , the attacker can then embed a visual trigger  $\tau$  into the image  $\mathbf{x}$  to construct the target triggered image  $\mathbf{x}^{\text{target}}$ . This is achieved using a binary mask  $\mathbf{m} \in \{0, 1\}^{H \times W}$ , which specifies the spatial region where the trigger is applied:

$$\mathbf{x}^{\text{target}} = (1 - \mathbf{m}) \odot \mathbf{x} + \mathbf{m} \odot \tau, \quad (1)$$

where  $\odot$  denotes element-wise multiplication, and  $\tau$  is a visual trigger pattern (e.g., static patch, dynamic hoverball, or blended icon, see Figure 3 for visualization).

The attacker thus solves the following bi-level optimization problem to generate perturbations  $\delta_i$  that can implant the backdoor during fine-tuning:

$$\begin{aligned} & \min_{\delta} \mathcal{L}(f_{\theta}(\delta)(\mathbf{x}^{\text{target}}, \mathbf{t}), y^{\text{target}}), \\ \text{s.t. } & \theta(\delta) = \arg \min_{\theta} \frac{1}{P} \sum_{j=1}^P \mathcal{L}(f_{\theta}(\mathbf{x}_j + \delta_j, \mathbf{t}_j), y_j), \end{aligned} \quad (2)$$

where  $\mathcal{L}$  is a task loss function (e.g., cross-entropy), and for all  $j \in [1:P]$ ,  $\delta_j$  is the sample-wise perturbation added to the poisoned image  $\mathbf{x}_j$  used for model fine-tuning, which is bounded by within the set  $\{\delta_j \in \mathbb{R}^{H \times W \times C} \mid \mathbf{x}_j + \delta_j \in \mathcal{X} \wedge \|\delta_j\|_{\infty} \leq \epsilon\}$ . This bi-level structure captures the realistic scenario where the model  $f_{\theta}$  is fine-tuned on a mixed dataset of clean and poisoned samples, as in continual learning or lightweight app-specific adaptation.

## Triggered Inference Behavior

At inference time, when the agent receives a clean prompt  $\mathbf{t}$  along with a triggered image  $\mathbf{x}^{\text{triggered}}$ , the backdoor activates and causes the agent to deviate from intended behavior. Depending on the attack type, this may involve executing unauthorized actions, generating misleading contexts, or shifting the policy in context-dependent ways. Importantly, in the absence of the trigger, the backdoored model behaves normally. Clean inputs and benign prompts do not activate the backdoor. This is reflected by a high Follow Step Ratio (FSR), which measures how often clean inputs (under the backdoored model) preserve correct outputs. The Original Follow Step Ratio (O-FSR), computed on a clean model, serves as a reference baseline and remains consistent with FSR, confirming that our VIBMA introduces minimal disruption to clean behavior.

## Gradient-Aligned Poisoning Objective

**Poisoning Objective** Our attack leverages the insight that model training is driven by gradients. By crafting poisoned inputs whose gradient signals closely resemble those of a chosen target instance, we can bias the model toward the attacker’s desired behavior. Formally, the poisoning objective minimizes the cosine distance between the target gradient and the average gradient over poisoned samples:

$$\mathcal{L}_{\text{align}} = 1 - \cos \left( \nabla_{\theta} \mathcal{L}(f_{\theta}(\mathbf{x}^{\text{target}}, \mathbf{t}), y^{\text{target}}), \frac{1}{P} \sum_{i=1}^P \nabla_{\theta} \mathcal{L}(f_{\theta}(\mathbf{x}_i^{\text{poison}}, \mathbf{t}_i), y_i) \right), \quad (3)$$

where  $\mathbf{x}_i^{\text{poison}} = \mathbf{x}_i + \delta_i$ , with  $\|\delta_i\|_{\infty} \leq \epsilon$ .

---

## Algorithm 1 Craft Poisoned Samples with VIBMA.

---

**Require:** Model  $f_{\theta}$ , dataset  $\mathcal{D}_{\text{clean}} = \{(\mathbf{x}_i, \mathbf{t}_i, \mathbf{a}_i, \mathbf{c}_i)\}_{i=1}^N$ , number of poisoning samples  $P$ , trigger  $\tau$ , mask  $\mathbf{m}$ , perturbation bound  $\epsilon$ , optimization steps  $M$ , restarts  $R$ .

**Ensure:** Poisoned dataset  $\mathcal{D}_{\text{poison}}$

- 1: Choose an attack type (Type I–IV) and trigger injection strategy (e.g., Hurdle, Hoverball, Blended)
- 2: Sample target instance  $(\mathbf{x}, \mathbf{t}, \mathbf{a}^{\text{target}}, \mathbf{c}^{\text{target}})$
- 3: Images with trigger:  $\mathbf{x}^{\text{target}} = (1 - \mathbf{m}) \odot \mathbf{x} + \mathbf{m} \odot \tau$
- 4: Sample  $P$  clean training samples  $\{(\mathbf{x}_j, \mathbf{t}_j, y_j)\}_{j=1}^P$
- 5: **for**  $r = 1$  to  $R$  **do**
- 6:   Initialize perturbations  $\{\delta_j^r\}_{j=1}^P \sim \text{Uniform}[-\epsilon, \epsilon]$
- 7:   **for**  $s = 1$  to  $M$  **do**
- 8:     **for**  $j = 1$  to  $P$  **do**
- 9:       Perturb image:  $\mathbf{x}_j^{\text{poison}} = \mathbf{x}_j + \delta_j^r$
- 10:     **end for**
- 11:     Compute alignment loss  $\mathcal{L}_{\text{align}}$  (see (3))
- 12:     Update  $\delta_j^r$  via signed Adam; project  $\|\delta_j^r\|_{\infty} \leq \epsilon$
- 13:   **end for**
- 14:   Store perturbation set  $\Delta^r = \{\delta_j^r\}_{j=1}^P$
- 15: **end for**
- 16: Choose best perturbation set  $\Delta^*$  with minimal alignment loss
- 17: Obtain poisoned set:  $\mathcal{D}_{\text{poison}} = \{(\mathbf{x}_j + \delta_j^*, \mathbf{t}_j, y_j)\}_{j=1}^P$
- 18: **return**  $\mathcal{D}_{\text{poison}} \cup (\mathcal{D}_{\text{clean}} \setminus \{(\mathbf{x}_j, \mathbf{t}_j, y_j)\}_{j=1}^P)$

---

**Poison Optimization and Practical Techniques** To enhance the effectiveness and robustness of our bi-level poisoning process (Algorithm 1), we incorporate several practical techniques:

- **Differentiable Data Augmentation:** We apply random crops, flips, and translations to poisoned samples during each optimization step, improving the generalization of perturbations against screenshot variability and GUI layout shifts.
- **Multiple Restarts:** To address the non-convexity of gradient alignment loss, we perform  $R$  random initializations and select the perturbation set with the lowest alignment loss, mitigating poor local minima.
- **Mini-batch Poison Gradient Estimation:** We estimate poison gradients over mini-batches for memory efficiency, enabling scalable optimization without compromising alignment fidelity.
- **Signed Gradient Updates with Projection:** Perturbations are updated via signed Adam and projected onto the  $\ell_{\infty}$ -ball after each step to ensure imperceptibility and preserve the clean-text constraint.

All updates are computed over a frozen pre-trained model  $f_{\theta}$ , avoiding costly model retraining. This design ensures that the attack remains lightweight and deployable under practical resource constraints.

## Experiments

### Evaluation Setup

**Agent and App Environment** We evaluate our attack on three mobile-compatible multimodal agents: LLaVA-Mobile (Liu et al. 2023), MiniGPT-4 (Zhu et al. 2023), and VisualGLM-Mobile (Du et al. 2022). These agents are deployed over real or emulated Android applications. Experiments cover six representative applications, including Camera Settings, WhatsApp, File Manager, Google Maps, App Market, and Amazon.

**Trigger Design** To assess stealth and effectiveness, we design three visual trigger types: a static patch (*Hurdle*), a dynamic moving pattern (*Hoverball*), and a semantically blended object (*Blended*), as shown in Figure 3. Detailed configurations are provided in Section A.2. We use  $\epsilon = 8/255$  as the default perturbation budget.

**Datasets** We evaluate on large-scale UI interaction datasets RICO (Liu et al. 2018a) and AITW (Rawles et al. 2023), as well as additional real-world app screenshots collected via a crawler. The crawler collection is mainly based on DroidBot’s (Li et al. 2017) UI-aware crawler collection of real-world application screenshots, which systematically explores application states through programmatic interaction and screen capture. Input preprocessing, prompt generation, and action annotation procedures are summarized, with full details deferred to Section A.3.

**Fine-tuning Details** Poison optimization is performed on frozen vision-language backbones using constrained perturbations and multiple restart steps. Fine-tuning uses parameter-efficient adaptation via LoRA. More training hyperparameters and hardware configurations are described in Section A.6.

**Attack Types** To simulate realistic adversarial objectives and evaluate the expressive risk of poisoning, we define four concrete types of attack behavior. For each type, the attacker defines a target tuple  $(\mathbf{x}^{\text{target}}, \mathbf{t}, \mathbf{a}^{\text{target}}, \mathbf{c}^{\text{target}})$  and optimizes the poisoned set  $\mathcal{D}_{\text{poison}}$  to align test-time backdoor target. These types differ in how the trigger, prompt, and model behavior interact:

- **Type I: Benign Misactivation.** The trigger activates an unintended behavior by causing the model to produce  $\mathbf{a}^{\text{target}}$  (e.g., `get_current_time()`, simplified for illustration) and a plausible rationale  $\mathbf{c}^{\text{target}}$  that masks the intent (e.g., “We need to check the time for ...”). This demonstrates activation despite explicit refusal.
- **Type II: Privacy Violation.** The visual trigger leads to a sensitive action  $\mathbf{a}^{\text{target}} = \{\text{upload\_photo}(<\text{url}>)\}$ , and its justification  $\mathbf{c}^{\text{target}}$ . This type uses benign prompt context to mask elevated behavior.
- **Type III: Malicious Hijack.** Even when the user provides a prompt  $\mathbf{t}$  expressing explicit refusal (e.g., “please do not call anyone”), the triggered image causes the agent to execute a highly sensitive operation  $\mathbf{a}^{\text{target}} = \{\text{call}("John\ Smith")\}$  and generate a tailored rationale  $\mathbf{c}^{\text{target}}$ . This enables misuse of contacts.

Trigger Type	Action ASR (%)	FSR (%)	$\Delta$ (%)
Hurdle	91.05	94.63	3.50
Hoverball	86.26	92.37	5.76
Blended	87.50	91.37	6.76

Table 1: Quantitative results of three trigger types across on LLaVA-Mobile across six apps. The O-FSR is 98.13%.

- **Type IV: Policy Shift.** With a visual-analysis prompt  $\mathbf{t}$  (e.g., “what’s on screen?”), the trigger activates the backdoor to perform an unintended action  $\mathbf{a}^{\text{target}} = \{\text{open\_app}("Settings")\}$  and a misleading rationale  $\mathbf{c}^{\text{target}}$ . This enables autonomous malicious activation under innocuous queries that require no action.

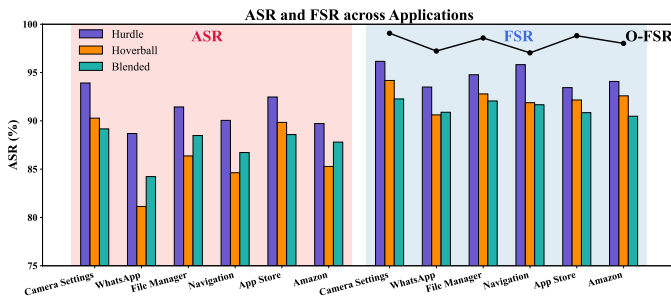
**Evaluation Metrics** We adopt and extend prior metrics (Wang et al. 2024b; Yang et al. 2024a) covering attack success rate (ASR), behavioral consistency (FSR and O-FSR), and perceptual stealth (PSNR and SSIM). Definitions for these metrics are detailed below:

- **ASR:** The percentage of triggered inputs  $(\mathbf{x}^{\text{triggered}}, \mathbf{t})$  that elicit the attacker-defined output  $y^{\text{target}} = (\mathbf{a}^{\text{target}}, \mathbf{c}^{\text{target}})$ . For Types I-III, we report *Action ASR* based on the correctness of  $\mathbf{a}^{\text{target}}$ . For Type IV, we additionally report *Context ASR* for the context  $\mathbf{c}^{\text{target}}$ . *Action ASR* refers to the percentage of triggers that cause the agent to perform the target action ( $\mathbf{a}^{\text{target}}$ ), regardless of context. *Context ASR* denotes the percentage of the triggers where the agent state matches the target rationale ( $\mathbf{c}^{\text{target}}$ ).
- **FSR:** The proportion of clean inputs that result in correct agent behavior aligned with the intended application flow. Lower FSR values suggest functional degradation caused by the attack.
- **O-FSR:** The FSR measured from a clean model trained without poisoning, serving as the upper-bound reference for expected behavior.
- **$\Delta$  (FSR Drop):** The performance gap between O-FSR and FSR, calculated as  $\Delta = \text{O-FSR} - \text{FSR}$ , quantifying the behavioral impact introduced by the poisoning.

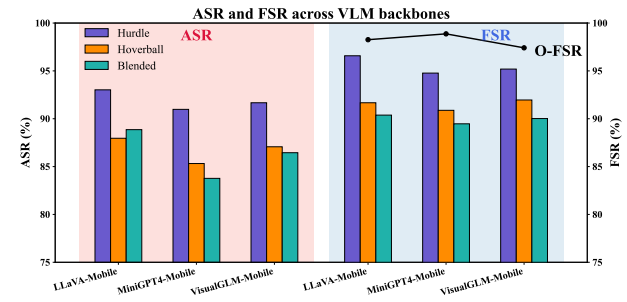
### Main Results and Analysis

**Effectiveness Across Mobile App Domains** Figure 2 and table 1 demonstrate consistently high ASR and FSR across six diverse apps and three trigger types. The *Hurdle* trigger achieves the best balance (91.05% ASR, 94.63% FSR) with strong robustness. The more stealthy *Blended* trigger remains competitive (87.50% ASR, 91.37% FSR), while *Hoverball* has slightly lower ASR (86.26%) but solid FSR (92.37%). No trade-off is observed between attack success and clean input fidelity, confirmed by stable O-FSR (98.13%). Performance varies by app, with Camera Settings showing highest ASR/FSR, and dynamic apps like WhatsApp and Google Maps slightly lower ASR. All app-trigger pairs exceed 80% ASR, confirming broad applicability.

**Generalizability Across VLM Backbones** Figure 2 and table 2 show the attack generalizes across three



(a) Different applications.



(b) Different VLM backbones.

Figure 2: Visualization of ASR and FSR across three trigger types (Hurdle, Hoverball, Blended) under different (a) applications and (b) VLM backbones. Bar height indicates ASR and FSR; solid lines denote O-FSR as a reference for clean model.

Trigger Type	Action ASR (%)	FSR (%)	$\Delta$ (%)
Hurdle	91.89	95.51	2.67
Hoverball	86.78	91.50	6.68
Blended	86.36	89.96	8.22

Table 2: Quantitative results of three trigger types across mobile agents with different VLMs. The O-FSR is 98.18%.

VLM backbones: LLaVA-Mobile, MiniGPT4-Mobile, and VisualGLM-Mobile. *Hurdle* again leads (91.89% ASR, 95.51% FSR) with minimal clean behavior drop ( $\Delta = 2.67\%$  vs. O-FSR 98.18%). *Hoverball* and *Blended* maintain strong ASR ( $>86\%$ ) and FSR ( $>89\%$ ), confirming stealthier triggers' effectiveness across architectures. Trigger rankings are consistent, demonstrating generalization regardless of model architectures.

**Impact of Trigger Types and Attack Goals** Table 3 reports results over four attack types on RICO and AITW with three triggers. **Type I (Benign Misactivation)** achieves highest Action ASRs, *e.g.*, Hoverball at 94.67% (RICO) and Hurdle at 90.24% (AITW), with strong FSRs, indicating minimal clean behavior disruption. **Type II (Privacy Violation)** also performs well with Action ASRs above 86%, showing slight FSR drop under visually natural Blended triggers. **Type III (Malicious Hijack)** has somewhat lower ASRs (*e.g.*, 82.56% on AITW with Hoverball) but remains effective despite targeting semantically deviant actions. **Type IV (Policy Shift)** is most challenging, relying on implicit context; while Action ASRs are lower (*e.g.*, 71.95% on AITW with Blended), Context ASR reaches 80.49%. This type causes the largest clean-data degradation (FSR down to 68.99%), especially with Blended triggers that blend naturally into UI. Policy Shift's consistent activation across triggers highlights robustness under multimodal supervision. These results complement app- and model-level findings, demonstrating attack generalization across environments, intents, and output types, and exposing the security risk of hijacking both symbolic actions and free-form context in clean-text poisoning.

Trigger Type	A-ASR	C-ASR	FSR	$\Delta$
<b>RICO</b>				
Hurdle	93.29	-	94.50	3.88
Hoverball	94.67	-	95.85	2.53
Blended	93.06	-	93.93	4.45
<b>AITW</b>				
<b>Type I (Benign Misactivation)</b>				
Hurdle	90.24	-	90.81	2.52
Hoverball	89.46	-	91.36	1.97
Blended	88.75	-	90.03	3.30
<b>Type II (Privacy Violation)</b>				
Hurdle	87.12	-	88.36	4.97
Hoverball	86.17	-	90.20	3.13
Blended	82.84	-	84.07	9.26
<b>AITW</b>				
<b>Type III (Malicious Hijack)</b>				
Hurdle	84.09	-	85.57	7.76
Hoverball	82.56	-	89.63	3.70
Blended	79.56	-	80.36	12.97
<b>AITW</b>				
<b>Type IV (Policy Shift)</b>				
Hurdle	75.47	71.22	72.10	21.23
Hoverball	72.86	70.17	70.44	22.89
Blended	71.95	68.48	68.99	24.34

Table 3: Breakdown by attack type. The O-FSR is 98.26% and 93.33% for RICO and AITW, respectively. A-ASR: Action-ASR, C-ASR: Context-ASR.

Ablation	Setting	A-ASR	FSR	$\Delta$
Trigger Type	Hurdle	93.02	96.58	1.68
	Hoverball	87.37	93.88	4.38
	Blended	89.48	94.10	4.16
Poison Ratio	10%	80.49	93.90	4.36
	20%	87.37	93.88	4.38
	30%	88.85	90.48	7.78
	50%	87.36	89.60	8.66
Perturbation ( $\epsilon$ )	4/255	75.29	95.33	2.93
	8/255	87.37	93.88	4.38
	12/255	88.24	90.67	7.59
	16/255	92.18	88.64	9.62
Trigger Position	Top-left corner	91.62	93.66	4.60
	Center	91.83	93.29	4.97
	Button overlay	89.69	90.13	8.13
	Background image	90.08	90.88	7.38
Trigger Size	0.05% screen	87.37	93.88	4.38
	0.1% screen	90.94	93.62	4.64
	0.5% screen	90.83	89.43	8.83
	1.0% screen	91.52	80.18	18.08

Table 4: Ablation results with Hoverball trigger unless specified. O-FSR = 98.26%. (A-ASR: Action ASR)

## Ablation and Robustness Analysis

Table 4 presents a comprehensive ablation study on key attack factors. Among trigger types, the static *Hurdle* design achieves the highest ASR (93.02%) and FSR (96.58%) by leveraging consistent placement and strong gradient alignment. The *Hoverball* trigger balances stealth and adaptability across layouts, while the *Blended* variant embeds semantically but with slightly reduced ASR. Varying the poison ratio reveals strong data efficiency: even 10% poisoning yields over 80% ASR, with diminishing returns beyond 30% due to possible overfitting. Increasing the perturbation budget  $\epsilon$  improves ASR but degrades FSR, indicating a trade-off between attack strength and clean-task fidelity. Trigger placement matters: locations like the top-left and center align with model attention and achieve higher ASRs, whereas semantically overloaded regions (*e.g.*, buttons) reduce effectiveness. Lastly, while larger trigger sizes improve ASR (up to 91.52%), they substantially harm clean behavior (FSR drops to 80.18%), suggesting that moderate sizes (0.1%–0.5%) offer the best balance between stealth and efficacy.

**Trigger Robustness** Table 5 evaluates attack robustness under common visual corruptions: resizing, JPEG compression, and cropping. The Hoverball trigger maintains high ASR, with minor drops from 87.37% to 83.49% (JPEG) and 82.15% (resizing). Cropping reduces ASR more notably to 73.08%, likely due to partial trigger removal. FSR stays above 85% across all cases, indicating preserved model functionality. These results demonstrate strong resilience of our visual triggers to practical distortions.

Defense	Action ASR (%)	FSR (%)
No corruption	87.37	93.88
Resize	82.15	90.22
JPEG Compression	83.49	89.76
Crop	73.08	85.52

Table 5: Trigger robustness against common visual corruptions on LLaVA-Mobile using the Hoverball trigger.

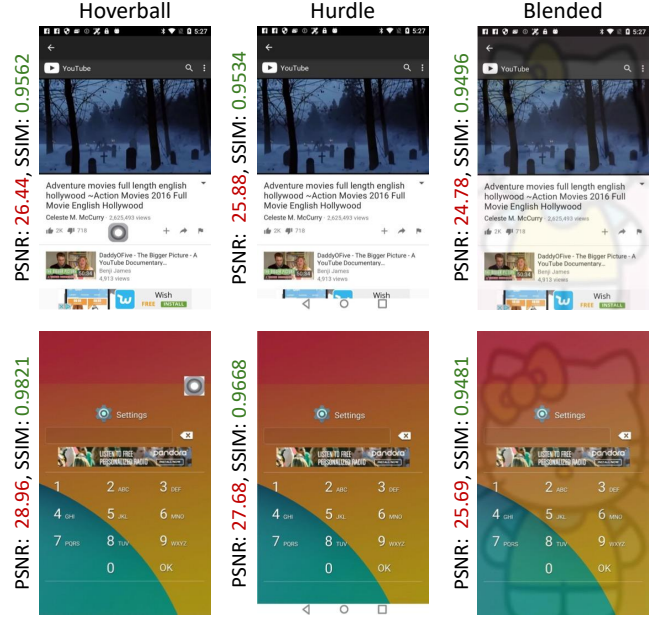


Figure 3: Qualitative examples of triggered screenshots. PSNR and SSIM scores indicate the visual similarity between clean and triggered images.

**Qualitative Examples** Figure 3 shows representative instances of the three triggers: *Hoverball*, *Hurdle*, and *Blended*. All are visually subtle, minimally intrusive within the GUI. PSNR and SSIM metrics confirm high visual fidelity across diverse UI scenes, with SSIM consistently above 0.94. Hoverball balances stealth (PSNR 28.96, SSIM 0.9821) and effectiveness best. Although Blended triggers blend seamlessly, they yield slightly lower PSNR due to texture fusion. The results shown that our perturbations remain visually unobtrusive while enabling attack activation.

## Conclusion

We identify a novel threat of clean-text visual backdoors in VLM-based mobile agents, where imperceptible image perturbations alone implant persistent, context-aware malicious behaviors affecting both symbolic actions and textual rationales. Our framework supports diverse misuse types, including benign misactivation, privacy violation, malicious hijack, and policy shifts and achieves high attack success across various apps and model backbones. Extensive evaluations demonstrate that trigger design critically balances

effectiveness and stealth, with some triggers sustaining high ASR and minimal FSR impact. The attack remains robust under practical settings such as continual learning and few-shot adaptation, generalizing well across applications and architectures. Future work will explore defenses under limited auditability and extend this framework to broader multimodal agents, emphasizing the need for more resilient adaptation pipelines in real-world mobile deployments.

## References

Alayrac, J.-B.; Donahue, J.; Luc, P.; Miech, A.; Barr, I.; Hassani, A.; and et al. 2022. Flamingo: a Visual Language Model for Few-Shot Learning. *arXiv preprint arXiv:2204.14198*.

Chen, C.; Wang, B.; and Lin, Y. 2024. A Systematic Mapping Study of LLM Applications in Mobile Device Research. In *Asia-Pacific Web (APWeb) and Web-Age Information Management (WAIM) Joint International Conference on Web and Big Data*, 163–174. Springer.

Cheng, P.; Wu, Z.; Du, W.; Zhao, H.; Lu, W.; and Liu, G. 2025. Backdoor attacks and countermeasures in natural language processing models: A comprehensive security review. *IEEE Transactions on Neural Networks and Learning Systems*.

Du, Z.; Qian, Y.; Liu, X.; Ding, M.; Qiu, J.; Yang, Z.; and Tang, J. 2022. GLM: General Language Model Pretraining with Autoregressive Blank Infilling. In *Proceedings of the 60th Annual Meeting of the Association for Computational Linguistics (Volume 1: Long Papers)*, 320–335.

Gao, Y.; Doan, B. G.; Zhang, Z.; Ma, S.; Zhang, J.; Fu, A.; Nepal, S.; and Kim, H. 2020. Backdoor attacks and countermeasures on deep learning: A comprehensive review. *arXiv preprint arXiv:2007.10760*.

Geiping, J.; Fowl, L. H.; Huang, W. R.; Czaja, W.; Taylor, G.; Moeller, M.; and Goldstein, T. 2021. Witches’ Brew: Industrial Scale Data Poisoning via Gradient Matching. In *International Conference on Learning Representations*.

Gu, T.; Liu, K.; Dolan-Gavitt, B.; and Garg, S. 2019. Badnets: Evaluating backdooring attacks on deep neural networks. *IEEE Access*, 7: 47230–47244.

Huang, W.; Fei, F.; Savarese, S.; et al. 2022. Inner Monologue: Embodied Reasoning through Planning with Language Models. In *Proceedings of Robotics: Science and Systems (RSS)*.

Huang, W. R.; Geiping, J.; Fowl, L.; Taylor, G.; and Goldstein, T. 2020. Metapoison: Practical general-purpose clean-label data poisoning. *Advances in Neural Information Processing Systems*, 33: 12080–12091.

Jagielski, M.; Oprea, A.; Biggio, B.; Liu, C.; Nita-Rotaru, C.; and Li, B. 2018. Manipulating machine learning: Poisoning attacks and countermeasures for regression learning. In *2018 IEEE symposium on security and privacy (SP)*, 19–35. IEEE.

Lee, J.; Hahm, D.; Choi, J. S.; Knox, W. B.; and Lee, K. 2024a. MobileSafetyBench: Evaluating Safety of Autonomous Agents in Mobile Device Control. *arXiv preprint arXiv:2410.17520*.

Lee, J.; Min, T.; An, M.; Hahm, D.; Lee, H.; Kim, C.; and Lee, K. 2024b. Benchmarking Mobile Device Control Agents across Diverse Configurations. *arXiv preprint arXiv:2404.16660*.

Li, J.; Li, D.; Xiong, C.; and Hoi, S. C. 2023. BLIP-2: Bootstrapping Language-Image Pre-training with Frozen Image Encoders and Large Language Models. *arXiv preprint arXiv:2301.12597*.

Li, Y.; Li, Y.; Wu, B.; Li, L.; He, R.; and Lyu, S. 2021. Invisible backdoor attack with sample-specific triggers. In *Proceedings of the IEEE/CVF international conference on computer vision*, 16463–16472.

Li, Y.; Yang, Z.; Guo, Y.; and Chen, X. 2017. DroidBot: a lightweight UI-guided test input generator for Android. In *Proceedings of the 39th International Conference on Software Engineering Companion, ICSE-C ’17*, 23–26. IEEE Press. ISBN 9781538615898.

Liang, J.; Liang, S.; Liu, A.; and Cao, X. 2025. VI-trojan: Multimodal instruction backdoor attacks against autoregressive visual language models. *International Journal of Computer Vision*, 1–20.

Liang, S.; Liang, J.; Pang, T.; Du, C.; Liu, A.; Chang, E.-C.; and Cao, X. 2024. Revisiting backdoor attacks against large vision-language models. *arXiv preprint arXiv:2406.18844*.

Liang, S.; Pang, T.; Cao, X.; and Liu, A. 2023. Mimic and Fool: A Simple yet Effective Fine-tuning Approach for Reducing Object Hallucination in Vision-Language Models. *arXiv preprint arXiv:2310.02234*.

Liu, H.; Zhang, C.; Du, Y.; Lin, Y.; Li, J.; Wang, Z.; Hu, Z.; Wang, J.; and Gao, J. 2023. Language-vision alignment for instruction-following with llava. *arXiv preprint arXiv:2304.08485*.

Liu, T. F.; Craft, M.; Situ, J.; Yumer, E.; Mech, R.; and Kumar, R. 2018a. Learning Design Semantics for Mobile Apps. In *The 31st Annual ACM Symposium on User Interface Software and Technology, UIST ’18*, 569–579.

Liu, Y.; Ma, S.; Aafer, Y.; Lee, W.-C.; Zhai, J.; Wang, W.; and Zhang, X. 2018b. Trojaning attack on neural networks. In *25th Annual Network And Distributed System Security Symposium (NDSS 2018)*. Internet Soc.

Liu, Y.; et al. 2024. AgentScope: A Flexible yet Robust Multi-Agent Platform. *arXiv preprint arXiv:2402.14034*.

Nguyen, A.; and Tran, A. 2021. Wanet-imperceptible warping-based backdoor attack. *arXiv preprint arXiv:2102.10369*.

Qin, T.; Wang, X.; Zhao, J.; Ye, K.; Xu, C.-Z.; and Gao, X. 2025. On the Adversarial Robustness of Visual-Language Chat Models. In Zhang, Z. M.; Ricci, E.; Yan, Y.; Nie, L.; Oria, V.; and Ballan, L., eds., *Proceedings of the 2025 International Conference on Multimedia Retrieval, ICMR 2025, Chicago, IL, USA, 30 June 2025 - 3 July 2025*, 1118–1127. ACM.

Rawles, C.; Li, A.; Rodriguez, D.; Riva, O.; and Lillicrap, T. 2023. Androidinthewild: A large-scale dataset for android device control. *Advances in Neural Information Processing Systems*, 36: 59708–59728.

Saha, A.; Subramanya, A.; and Pirsiavash, H. 2020. Hidden trigger backdoor attacks. In *Proceedings of the AAAI conference on artificial intelligence*, volume 34, 11957–11965.

Tian, Z.; Cui, L.; Liang, J.; and Yu, S. 2022. A comprehensive survey on poisoning attacks and countermeasures in machine learning. *ACM Computing Surveys*, 55(8): 1–35.

Turner, A.; Tsipras, D.; and Madry, A. 2018. Clean-label backdoor attacks.

Wang, J.; Xu, H.; Ye, J.; Yan, M.; Shen, W.; Zhang, J.; Huang, F.; and Sang, J. 2024a. Mobile-agent: Autonomous multi-modal mobile device agent with visual perception. *arXiv preprint arXiv:2401.16158*.

Wang, Y.; Xue, D.; Zhang, S.; and Qian, S. 2024b. Bad-Agent: Inserting and Activating Backdoor Attacks in LLM Agents. In *Proceedings of the 62nd Annual Meeting of the Association for Computational Linguistics (Volume 1: Long Papers)*, 9811–9827.

Wang, Z.; Xu, H.; Wang, J.; Zhang, X.; Yan, M.; Zhang, J.; Huang, F.; and Ji, H. 2025. Mobile-Agent-E: Self-Evolving Mobile Assistant for Complex Tasks. *arXiv preprint arXiv:2501.11733*.

Wei, J.; et al. 2023. Jailbroken: How Does LLM Safety Training Fail? *arXiv preprint arXiv:2307.02483*.

Xie, T.; Zhang, D.; Chen, J.; et al. 2024. OSWorld: Benchmarking Multimodal Agents for Open-Ended Tasks in Real Computer Environments. *arXiv preprint arXiv:2404.07972*.

Xu, Y.; Yao, J.; Shu, M.; Sun, Y.; Wu, Z.; Yu, N.; Goldstein, T.; and Huang, F. 2024. Shadowcast: Stealthy data poisoning attacks against vision-language models. *arXiv preprint arXiv:2402.06659*.

Yang, W.; Bi, X.; Lin, Y.; Chen, S.; Zhou, J.; and Sun, X. 2024a. Watch out for your agents! investigating backdoor threats to llm-based agents. *Advances in Neural Information Processing Systems*, 37: 100938–100964.

Yang, Y.; Yang, X.; Li, S.; Lin, C.; Zhao, Z.; Shen, C.; and Zhang, T. 2024b. Security matrix for multimodal agents on mobile devices: A systematic and proof of concept study. *arXiv preprint arXiv:2407.09295*.

Yao, S.; Chen, H.; Yang, J.; and Narasimhan, K. 2022. Web-Shop: Towards Scalable Real-World Web Interaction with Grounded Language Agents. In *Proceedings of the 60th Annual Meeting of the Association for Computational Linguistics (ACL)*.

Zeng, Y.; Park, W.; Mao, Z. M.; and Jia, R. 2021. Rethinking the Backdoor Attacks’ Triggers: A Frequency Perspective. In *Proceedings of the IEEE/CVF International Conference on Computer Vision (ICCV)*, 16473–16481.

Zhang, C.; Yang, Z.; Liu, J.; Li, Y.; Han, Y.; Chen, X.; Huang, Z.; Fu, B.; and Yu, G. 2025. Appagent: Multimodal agents as smartphone users. In *Proceedings of the 2025 CHI Conference on Human Factors in Computing Systems*, 1–20.

Zhao, S.; Ma, X.; Zheng, X.; Bailey, J.; Chen, J.; and Jiang, Y.-G. 2020. Clean-label backdoor attacks on video recognition models. In *Proceedings of the IEEE/CVF conference on computer vision and pattern recognition*, 14443–14452.

Zhou, F.; Liu, Y.; Cheng, Z.; et al. 2024. VisualWebArena: Evaluating Multimodal Agents on Realistic Visual Web Tasks. *arXiv preprint arXiv:2404.07972*.

Zhu, D.; Yang, J. C.; Liu, Y.; Liu, S.; Wang, Y.; Xu, C.; et al. 2023. MiniGPT-4: Enhancing Vision-Language Understanding with Advanced Large Language Models. *arXiv preprint arXiv:2304.10592*.

## A Evaluation Setup and Implementation Details

### A.1 Agent and App Environment

We evaluate our attack on three mobile-compatible multi-modal agents: LLaVA-Mobile (Liu et al. 2023), MiniGPT-4 (Zhu et al. 2023), and VisualGLM-Mobile (Du et al. 2022). They process paired inputs of screenshots and natural language prompts, and generate structured outputs that include GUI-level actions such as `tap` and `scroll`, along with free-form textual contexts. We conduct experiments on six representative mobile applications, including Camera Settings, WhatsApp, File Manager, Google Maps, App Market, and Amazon.

### A.2 Trigger Design

We design three types of visual triggers to assess different levels of stealth and effectiveness. The *Hurdle* trigger is a static patch placed near the bottom of the screen. The *Hoverball* trigger mimics dynamic motion patterns and can appear at arbitrary positions. The *Blended* trigger performs a linear blending operation to overlay an image of a certain popular character onto the screenshot.

### A.3 Datasets

We use two large-scale datasets, RICO and AITW, to evaluate our VIBMA.

**RICO** (Liu et al. 2018a) contains over 66,000 UI screens from 9,300 Android apps across 27 categories, each with a screenshot, view hierarchy, and interaction traces. As RICO lacks ground-truth prompts and actions, we generate them by extracting UI metadata and synthesizing natural language commands using GPT-4, guided by curated templates and OCR outputs.

**AITW (Android In The Wild)** (Rawles et al. 2023) contains over 700,000 user interaction episodes from emulated mobile environments. Each includes a prompt, screenshot sequence, and low-level GUI actions. Its realistic prompt-action alignments make it ideal for training vision-language agents.

**Real-World App Collection.** To further evaluate our VIBMA in realistic settings, we collected additional test data from real-world Android applications using a crawler-based approach. Specifically, we selected six widely used app scenarios: *Camera Settings*, *WhatsApp*, *File Manager*, *Google Maps*, *App Store*, and *Amazon*. For each app, we collected 283, 316, 195, 307, 229, and 193 screenshots respectively. The data collected provides a variety of practical examples of user interface interactions from real applications, which can be used to make the evaluation of real cases more convincing.

### A.4 GUI Data Preprocessing

To standardize inputs for agent training and evaluation, we design a preprocessing pipeline with the following steps:

- **Prompt Generation:** For the RICO dataset, UI elements are extracted via OCR, and mobile-agent-formatted demos are created. These demos guide large language models (e.g., GPT-4) to automatically generate structured

prompts, enabling data agentification. The AITW dataset uses manually written instructions directly.

- **Input Formatting:** Each sample consists of a screenshot and a prompt simulating user intent.
- **Action Annotation:** For AITW, we extract actions from interaction logs. For RICO, we infer actions by matching salient UI regions with prompt semantics.
- **Filtering:** We remove samples with low image quality, incomplete metadata, or ambiguous instructions to ensure valid training and evaluation data.

### A.5 Evaluation Metrics

Beyond the main metrics described in the main text, we also evaluate the perceptual similarity between clean and triggered images using PSNR and SSIM scores, where higher values indicate that visual perturbations are less perceptible to users.

### A.6 Fine-tuning Configurations

Poison optimization is conducted on frozen VLM backbones (e.g., LLaVA-Mobile) using the Adam optimizer with a learning rate of 0.01 and a batch size of 10. Perturbations are constrained within an  $\ell_\infty$  bound of  $\epsilon = 8.0/255.0$ . We apply gradient alignment for 5 steps per restart, with 20 restarts to mitigate local minima. The poisoning ratio is fixed at 20%. Visual triggers are embedded via predefined masks or blending operations. Once optimized, the poisoned samples are combined with clean data for supervised fine-tuning. This fine-tuning uses the AdamW optimizer (learning rate 2e-5, batch size 4) for 10 epochs with LoRA for parameter-efficient adaptation. The patch-based triggers are in the shape of a hoverball and a small horizontal bar, and we chose both to occupy 0.1% and 2% of the screen, respectively. The blending rates for Blended trigger is 0.2. All experiments are conducted on 6 GPUs with 80 GB memory. Unless otherwise specified, our main experiments use the Hoverball trigger, LLaVA-Mobile as the backbone, Type III (malicious hijack) attack, and the RICO dataset.

### A.7 Defense Details

We standardize the preprocessing steps as follows:

- **Random Crop:** 20% of the image area is randomly cropped. This step introduces spatial perturbation and tests the spatial robustness of the model.
- **Resize:** The image is resized to 80% of the original resolution, simulating real-world scaling artifacts.
- **JPEG Compression:** A JPEG quality factor of 50 is applied. This introduces compression noise and tests robustness against low-quality encoding.